Science Advances

AAAS

advances.sciencemag.org/cgi/content/full/3/6/e1700314/DC1

Supplementary Materials for

High particulate iron(II) content in glacially sourced dusts enhances productivity of a model diatom

Elizabeth M. Shoenfelt, Jing Sun, Gisela Winckler, Michael R. Kaplan, Alejandra L. Borunda, Kayla R. Farrell, Patricio I. Moreno, Diego M. Gaiero, Cristina Recasens, Raymond N. Sambrotto, Benjamin C. Bostick

Published 23 June 2017, *Sci. Adv.* **3**, e1700314 (2017)
DOI: 10.1126/sciadv.1700314

This PDF file includes:

Supplementary Materials

table S1. Name, type, location, and description, with references if applicable, for each sediment sample used in this study.

GLACIOGENIC			
Sample	latitude	longitude	Description
Lago Eberhard, 680 cm	-51.6100	-72.6300	Coarse layer in glacio-lacustrine sediment, deposited (~16,000 years ago) after ice recession, near Puerto Natales. Inferred to be either a glacier meltwater plume or ice rafted debris layer (*85*)
Lago Eberhard, 730 cm	-51.6100	-72.6300	Coarse layer in glacio-lacustrine sediment, deposited (~16,000 years ago) after ice recession, near Puerto Natales. Inferred to be either a glacier meltwater plume or ice rafted debris layer (*85*)
MK2	-50.9542	-72.7932	Glacio-lacustrine sediment reworked within till, in Torres del Paine. Essentially, glacial 'rock flour' deposited in a large proglacial lake that was dammed by the remnant Patagonian ice sheet ~14,000 years ago, that was then reworked into a glacial deposit during an advance (*86*)
MK3	-50.9644	-72.7889	Glacio-lacustrine sediment (rock flour) on top of a Late Glacial moraine in Torres del Paine. A large proglacial lake that was dammed by the remnant Patagonian ice sheet <14,000 years ago (*86*)
MK6	-49.9790	-73.3103	Sediment from a modern moraine in the Upsala glacier area in the Lago Argentino basin. This 1973 moraine is at the entrance to Agassiz Este valley. We sampled the moraine matrix (finer) (*71*)
PMG	-50.4901	-73.0542	Sediment in the Perito Moreno Glacier in the Lago Argentino basin. This is sediment coming out of the glacier today (modern glaciogenic sediment source)
SAF15	-50.7160	-73.0744	Sediment from a relatively recent moraine formed by the Frías glacier in the Lago Argentino basin. We sampled the moraine matrix (finer) near a 140 year 10-Be age (*87*)
SLG	-47.4822	-72.3651	Sediment from a moraine in the San Lorenzo area. Late Glacial in age
SMD13-3	-52.9096	-70.0337	Sediment from a large outwash plain headed towards the South Atlantic Ocean, ~20,000 years old (*72*), in the Strait of Magellan area. The sample was from a gravel pit close to where a moraine transitions to the outwash
NON-GLACIOGENIC			
Sample	latitude	longitude	Description
Cardiel 1014 (CAR14)	-48.8597	-71.0579	Sediments deposited during former high stand (+45 m) of Lago Cardiel, Patagonia. The sediments are at 304m elevation and Holocene in age (*73*)
Cardiel 1019 (CAR19)	-48.9530	-71.0783	Sediments deposited during former high stand (+55 m) of Lago Cardiel, Patagonia. The samples are at 312m elevation and Holocene in age (*73*)
Fenix VB	-46.6313	-70.9629	From a dust trap set up on a moraine. Modern material material blown into the dust trap over a 2 year period (*88, 89*)
Lago Argentino 1	-50.2034	-71.9372	Sample collected from a dune like feature at the end of Lago Argentino (*89*)
SAF2	-30.61	-69.06	Sample collected from dry lakebed at Barriales, Central West Argentina (*89*)
SAF3	-27.02	-66.51	Sample collected from alluvial fan, Campo Arenal, Puna (*89*)
SAF5	-23.60	-65.86	Sample collected from dry lakebed, Guayatayoc, Puna (*89*)
SAF10	-29.29	-67.51	Sample collected from alluvial fan, Nonogasta, Central West Argentina (*89*)

table S2. LCF results for samples. Mineral components, Fe(II), and solubility based on linear combination fitting of XAS spectra. Analytical errors are those reported by Sam Webb's SIXPack software, and propagated for Fe(II) percentage based on the Fe(II) content of the pure mineral structure. We considered hornblende to contain 50% Fe(II), 50% Fe(III). Fe content for sediments used in cultures include weight % Fe(II) content from XRF data (see Methods).

GLACIOGENIC						
Sample	**hematite**	**magnetite**	**siderite**	**ferrihydrite**	**goethite**	
Lago Eberhard, 680 cm	0.33±2.0%	0.0±3.4%	14.7±5.6%	8.4±9.0%	0.1±6.2%	
Lago Eberhard, 730 cm	0.21±2.4%	0.0±4.2%	20.2±6.8%	25.8±11.0%	0.0±7.6%	
MK2	2.5±1.6%	0.7±2.7%	22.5±4.3%	36.4±6.9%	0.0±4.8%	
MK3	0.64±2.1%	1.9±2.9%	6.8±3.6%	39.9±9.4%	0.0±4.2%	
MK6 (2.8wt% Fe)	0.37±2.7%	0.0±4.7%	37.4±7.6%	0.0±12.2%	0.0±8.4%	
PMG (1.8wt% Fe)	0.36±2.4%	0.0±3.6%	7.1±4.1%	22.3±12.0%	0.0±5.2%	
SAF15	1.0±3.0%	0.0±4.3%	0.0±5.1%	7.1±14.9%	14.9±6.4%	
SLG	9.5±3.0%	0.0±4.1%	0.1±5.1%	26.3±13.3%	0.2±6.0%	
SMD13-3 (16wt% Fe)	0.0±1.9%	0.7±2.6%	3.4±3.3%	46.3±8.6%	0.0±3.9%	
GLACIOGENIC (cont.)						
Sample	**pyrite**	**glauconite**	**biotite**	**hornblende**	**Fe(II)**	**Cumulative solubility**
Lago Eberhard, 680 cm	0.0±1.2%	14.1±3.9%	19.5±3.9%	42.9±5.5%	56±8%	2.7%
Lago Eberhard, 730 cm	4.0±1.5%	1.6±4.7%	33.6±4.8%	14.6±6.7%	65±9%	2.6%
MK2	1.8±0.9%	0.7±3.0%	15.6±3.1%	19.8±4.2%	50±6%	2.5%
MK3	1.7±1.1%	1.5±3.5%	19.3±3.7%	28.3±4.3%	43±6%	2.0%
MK6 (2.8wt% Fe)	4.1±1.6%	0.0±5.3%	45.4±5.4%	12.7±7.5%	93±10%	3.4%
PMG (1.8wt% Fe)	0.0±1.2%	0.0±4.9%	34.1±4.3%	36.1±5.2%	59±7%	2.3%
SAF15	1.9±1.6%	5.5±5.7%	21.6±5.4%	48.0±6.2%	48±8%	2.1%
SLG	6.6±1.5%	17.8±5.1%	21.6±5.2%	17.9±6.1%	37±8%	1.9%
SMD13-3 (16wt% Fe)	0.0±1.0%	0.1±3.3%	18.2±3.3%	31.4±3.9%	37±5%	1.8%
NON-GLACIOGENIC						
Sample	**hematite**	**magnetite**	**siderite**	**ferrihydrite**	**goethite**	
Cardiel 1014 (CAR14, 3.3wt% Fe)	0.07±2.1%	0.2±3.2%	0.0±3.6%	28.4±10.8%	4.2±4.6%	
Cardiel 1019 (CAR19, 1.8wt% Fe)	2.3±1.8%	0.0±3.0%	0.0±4.9%	23.9±7.9%	16.3±5.5%	
Fenix VB	8.0±2.2%	2.0±3.9%	0.0±6.3%	61.1±10.2%	0.0±7.0%	
Lago Argentino 1	11.1±2.1%	3.9±3.6%	0.0±5.9%	36.5±9.4%	6.1±6.5%	
SAF2	5.1±1.7%	0.0±2.5%	0.0±2.9%	32.9±8.6%	13.9±3.7%	
SAF3	4.6±2.3%	3.8±3.3%	0.0±3.87%	37.7±11.4%	0.0±4.9%	
SAF5	10.1±2.3%	0.0±3.2%	2.0±3.8%	41.6±11.2%	1.5±4.9%	
SAF10	10.6±2.2%	0.0±3.2%	0.0±3.6%	47.7±10.7%	4.7±4.7%	
NON-GLACIOGENIC (cont.)						
Sample	**pyrite**	**glauconite**	**biotite**	**hornblende**	**Fe(II)**	**Cumulative solubility**
Cardiel 1014 (CAR14, 3.3wt% Fe)	0.0±1.1%	28.7±4.0%	0.0±3.9%	38.4±4.6%	19±6%	1.8%
Cardiel 1019 (CAR19, 1.8wt% Fe)	0.1±1.1%	32.7±3.4%	0.0±3.6%	24.8±4.9%	12±7%	1.4%
Fenix VB	0.0±1.4%	5.0±4.4%	0.0±4.5%	23.9±6.3%	13±9%	1.3%
Lago Argentino 1	0.2±1.2%	8.2±4.0%	3.4±4.1%	30.6±5.7%	20±8%	1.4%
SAF2	1.5±0.9%	16.4±3.3%	9.4±3.1%	20.8±3.5%	21±5%	1.4%
SAF3	0.0±1.2%	28.2±4.3%	0.0±4.1%	25.8±4.7%	14±6%	1.5%
SAF5	0.0±1.2%	14.0±4.1%	5.6±4.1%	25.2±4.7%	20±6%	1.5%
SAF10	0.0±1.1%	11.9±4.0%	2.0±3.9%	23.0±4.5%	14±6%	1.3%

table S3. Principal component loadings. Loadings per sample/standard of principal components generated from samples. Standards are not included in the generation of the components. The Fe(II) content by percent of total Fe (%Fe(II)) is also listed. Errors are 67% confidence intervals based on the calibration curve (fig. S2).

GLACIOGENIC							
Sample	**pc1**	**pc2**	**pc3**	**pc4**	**pc5**	**pc6**	**Fe(II)**
Lago Eberhard, 680 cm	-21.03	-10.83	-1.56	-2.37	-3.04	-3.00	59±11%
Lago Eberhard, 730 cm	-19.55	-15.42	-1.78	-2.89	-1.23	-0.27	69±12%
MK2	-18.23	-8.44	-1.59	-2.31	0.79	1.01	54±11%
MK3	-21.42	-12.06	4.04	-3.36	-0.41	1.41	61±11%
MK6	-17.26	-21.34	-3.77	-0.11	-7.82	-3.79	81±12%
PMG	-20.46	-19.58	4.97	10.24	1.07	7.44	78±12
SAF15	-21.25	-8.67	0.79	5.99	0.90	-7.41	54±11%
SLG	-26.15	-5.36	4.65	1.21	6.62	-1.76	47±11%
SMD13-3	-18.95	-9.07	3.94	-1.16	0.15	0.17	55±11%
NON-GLACIOGENIC							
Sample	**pc1**	**pc2**	**pc3**	**pc4**	**pc5**	**pc6**	**Fe(II)**
Cardiel 1014 (CAR14)	-39.32	24.22	14.17	3.48	-7.25	-1.03	-17±12%
Cardiel 1019 (CAR19)	-30.41	11.15	3.62	-4.88	-0.91	0.68	11±11%
Fenix VB	-17.34	4.42	-2.00	-2.43	5.52	1.21	26±11%
Lago Argentino 1	-17.49	2.25	-2.13	-3.63	0.35	4.36	31±11%
SAF2	-27.10	6.20	0.39	-1.46	6.19	-0.60	22±11%
SAF3	-30.16	13.22	-7.75	3.92	-0.65	6.07	7±11%
SAF5	-26.38	6.43	-13.68	-0.51	-5.50	2.90	22±11%
SAF10	-30.66	12.71	-9.86	4.89	3.45	-7.12	8±11%
STANDARDS							
Sample	**pc1**	**pc2**	**pc3**	**pc4**	**pc5**	**pc6**	**Fe(II)**
hematite	-19.55	19.60	-4.51				0%
glauconite	-31.66	15.08	1.82				0%
goethite	-24.49	13.88	-2.40				0%
magnetite	-19.06	5.75	-1.34				33%
hornblende	-22.65	-11.98	5.68				50%
biotite	-16.04	-28.91	1.96				100%

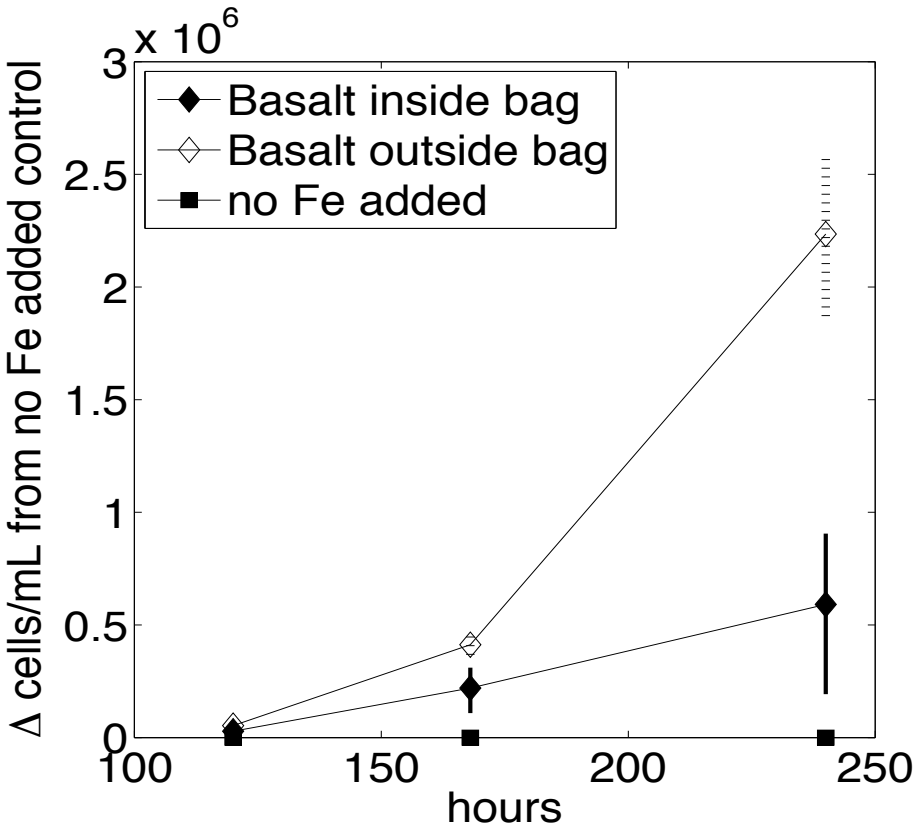

fig. S1. Dialysis bag experiments with *P. tricornutum*. Growth curves for *P. tricornutum* exposed to 0.1 g/L basalt particulates (2.0 m^2 surface area/g) both inside and outside of bags made with 1% w/v EDTA-cleaned 2000 Da dialysis tubing. The samples with basalt in bags (filled diamonds), basalt outside of bags (open diamonds), and 'no Fe added' control (filled squares) all contained dialysis bags for consistency. Cultures were inoculated to 2000 cells/mL at the beginning of the experiment and cells were placed outside of the dialysis bags such that when the basalt was outside of the bags, direct contact between particulates and diatoms was allowed. These cultures were grown in typical f/2 media with natural coastal seawater and no EDTA, so the relatively high growth in the 'no Fe added' control was subtracted from the rest of the data. Error bars represent the range of values for the experiments run in triplicate (solid error bars) and duplicate (hashed error bars). The 'no Fe added' control is included in the plot to emphasize that these are all differences from the control, since control growth was not zero. The control culture reached a cell density of about 1.2 million cells by the final data point of the experiment. Diatom growth was higher when basalt was added outside the dialysis bag versus inside the dialysis bag for this experiment and an additional three similar experiments, not shown. In a separate experiment, soluble $FeCl_3$ added to the inside of a dialysis bag was used to confirm that soluble Fe reached a quick equilibrium with the media outside the bag.

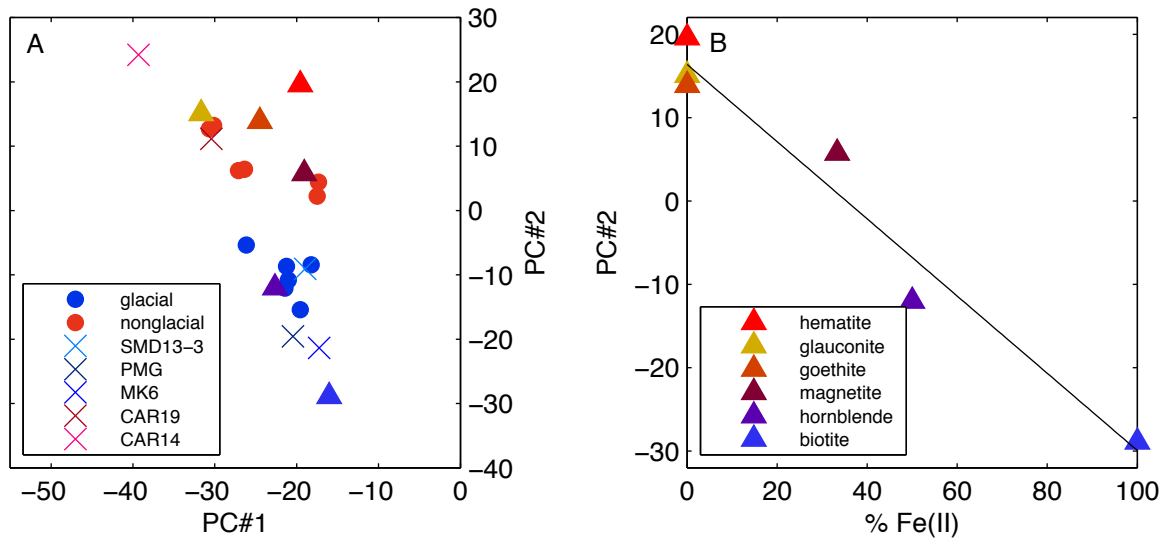

fig. S2. Principal component loadings versus Fe(II) content for reference standards and samples. (**A**) Principal components #1 versus #2 for each sample and (**B**) reference standard calibration curve of Fe content, %Fe(II), versus PC#2 loadings used to calculated %Fe(II) for the samples.

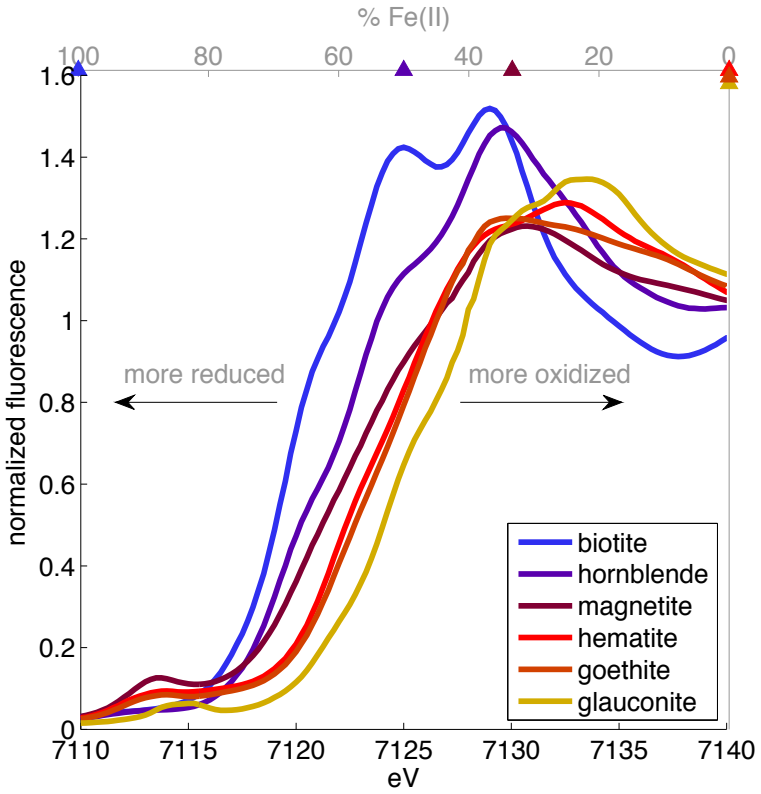

fig. S3. Subset of reference spectra used for LCF that were also used for PCA, with Fe(II) content. The spectra are plotted on the black x and y axes. The Fe(II) content for each mineral is plotted on the grey x axis at the top of the plot, and is based on the structure of the pure mineral.